Free-surface adjustment and topographic waves in coastal currents

By E. R. JOHNSON[1] AND M. K. DAVEY[2]

[1] Department of Mathematics, University College London, Gower Street,
London WC1E 6BT, UK

[2] Meteorological Office Unit, Hooke Institute for Atmospheric Research, Clarendon Laboratory,
Parks Road, Oxford OX1 3PU, UK

The adjustment of rotating free-surface flow over a step-like escarpment abutting a vertical wall is discussed in the context of the shallow-water equations. The problem is simplified by considering an escarpment of small fractional depth, so that on the slow topographic timescale the initial, fast Poincaré and Kelvin wave adjustment of the free surface is effectively instantaneous, and further simplified by considering the surface displacement to be small compared with the escarpment height so that particle velocities are negligible during the topographic adjustment. Direct solution of the resulting linear system is not straightforward as arbitrarily small-scale motions are generated at sufficiently large times. The problem is reduced by a Green's function technique to one spatial dimension and the wall boundary layers resolved by introducing a scaling based on previously obtained limit solutions. Solutions verify the information-propagation arguments of Johnson (1985) and Gill *et al.* (1986) and also show interchange of fluid across the escarpment as eddies formed as the current crosses the step travel along the step with shallow water to their right. The pattern of evolution of the system is independent of the direction of the flow, depending solely on the sign of the topographic step. If the escarpment is such that topographic waves travel away from the wall, then a tongue of fluid moves outward along the step: the initial jet along the wall is diverted to flow parallel to, rather than across, the step. If waves travel towards the wall then the current is pinched into the wall and fluid crosses the escarpment in a thinning jet.

1. Introduction

Long topographic waves in the ocean propagate with shallow water to their right (in the Northern hemisphere). This introduces an asymmetry into the evolution of flows above uneven bathymetry. In particular, flow forced over a rectilinear step deviates in opposite directions depending on whether the step is upwards or downwards. For infinitely long rectilinear ridges or steps the linear evolution of the flow can be followed straightforwardly by a Fourier superposition of the wave modes supported by the topography, and no singularities develop. A closed-form example of this is given in §3.

In the oceans and the laboratory rectilinear topography cannot extend indefinitely and is eventually interrupted by sidewalls of the ocean basin or rotating vessel. Energy carried towards the wall by long waves is in general reflected as short waves. At large time the flow is dominated by the waves of lowest frequency and the energy contained in the reflected waves is increasing confined to the neighbourhood of the

sidewall. The straightforward decomposition of arbitrary initial conditions into the propagating modes found over infinitely long topography is no longer possible, and an unsteady boundary layer forms at the wall.

This development is especially simple above topography consisting of a single vertical escarpment. There is then no reversal of group velocity for short waves, energy propagation is unidirectional, and so energy carried towards a wall accumulates there, forming a singularity at infinite time. The topographic waves in this limit are double Kelvin waves (Longuet-Higgins 1968; Rhines 1969).

This latter geometry has been considered in Johnson (1985) (called I herein) and Gill *et al.* (1986) (called II herein). Paper II considers the evolution of the free surface of a shallow layer of fluid confined in a semi-infinite domain by a vertical sidewall with topography consisting of a vertical escarpment perpendicular to the wall. The initial surface profile is taken to be a single step parallel to the sidewall (figure 1): in the absence of topography the free surface adjusts to geostrophy, in a time of order the inertial period, to give an alongshore current (i.e. a flow parallel to the wall). Steady solutions are obtained in II using the unidirectional propagation of information to infer that if the escarpment is such that long waves travel outwards then the eventual surface elevation over the escarpment coincides with that initially at the wall, whereas if long waves travel inwards the eventual elevation over the escarpment is that initially far from the wall, i.e. zero. This information argument is supported in II by time-dependent numerical integrations of finite-difference approximations to the two-dimensional equations of motion. For inwardly propagating waves at sufficiently large times these integrations are unable to resolve the increasingly small scales generated near the wall–step junction. A rigorous justification of the argument is given in I for the rigid-lid limit of infinite deformation radius where conformal mapping allows the domain to be transformed into one in which the evolution can be described in closed form by a Fourier superposition of modes. Asymptotic evaluation of the resulting integrals verifies the information propagation argument.

It is the purpose of the present paper to describe the transient development of the steady flows discussed in II without restriction to the rigid-lid limit. The solution combines the developing singularity of I with the finite speed of propagation and confinement of the flow in II. Section 2 shows that for topography of small fractional height two distinct timescales emerge. The linear shallow-water equations reduce to a fast, inertial-timescale system describing the adjustment to geostrophy of the initial unbalanced surface displacement and a slow, vortex-stretching-timescale system describing the subsequent evolution of this now geostrophic state. The topographic evolution over an escarpment is shown to be particularly simple, satisfying a steady Helmholtz equation in a quarter-plane with time-dependent boundary conditions. Section 3 gives the closed-form solution obtained by Fourier superposition for an infinitely long escarpment and presents an alternative derivation using a Green's function representing free-surface point vortices. This reduces the problem to an integral equation in one spatial dimension which is easily integrated numerically. The method is not restricted to infinite domains and in §4 it is applied to the more difficult problem with a bounding wall. Knowledge of solutions close to and far from the wall leads to the introduction of a stretched coordinate system that resolves the short lengthscales present when energy is incoming. The results are discussed briefly in §5.
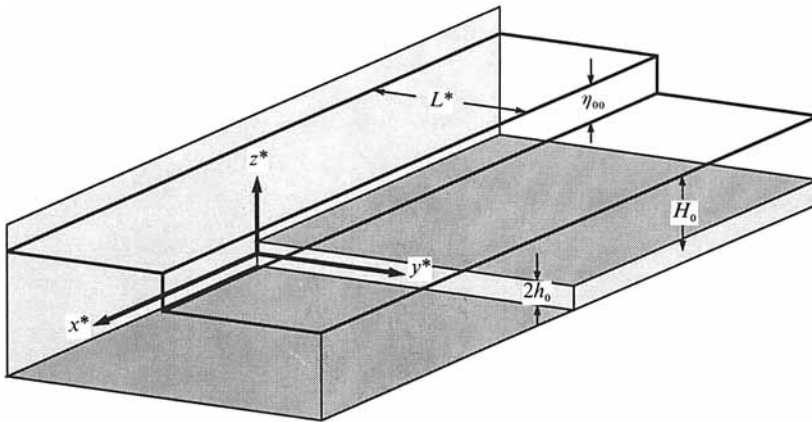
FIGURE 1. The geometry considered and the initial surface profile. The domain is semi-infinite with average depth H_0 and a rigid vertical wall at $y^* = 0$. An escarpment (later taken to be vertical) of height $2h_0$ stretching perpendicularly away from the wall is present on the lower boundary. Initially the free surface has a discontinuity of height η_{00} along the line $y^* = L^*$ parallel to the wall.

2. Governing equations

Consider a horizontally semi-infinite layer of incompressible inviscid homogeneous fluid of average depth H_0 rotating as a rigid body with constant angular velocity Ω about a vertical axis. Take Cartesian axes $Ox^*y^*z^*$ so that the bounding vertical wall is given by $y^* = 0$ and the rigid lower boundary by $z^* = h_0 h(x^*/L^*)$ where h is order one. Measure the deviation, from the horizontal plane $z^* = H_0$, of the free surface by η^*, and let the free surface initially have a downward step from $\eta^* = \eta_{00}$ in $0 < y^* < L^*$ to $\eta^* = 0$ in $y^* > L^*$. This geometry (figure 1) is the same as in II. As in the classical work of Rossby (1937 *a*, *b*), the free surface adjusts to geostrophy in a time of order the inertial period $(2\Omega)^{-1}$. The geostrophic flow has lengthscale of order the Rossby radius, $a = (gH_0)^{\frac{1}{2}}/2\Omega$ and velocity of order $U = g\eta_{00}/2\Omega a$. Topographic compression of vortex filaments generates vorticity of order $2\Omega\epsilon$, where $\epsilon = h_0/H_0$, and so introduces a second, topographic vortex-stretching, timescale $T = (2\Omega\epsilon)^{-1}$ (Johnson 1984). This timescale is long compared with the inertial time provided $\epsilon \ll 1$ and short compared with the advection time a/U provided $\eta_{00}/h_0 \ll 1$. Under these conditions the classical Rossby adjustment is fast, followed by a slow, evolution controlled by topographic waves of timescale T before advection becomes important.

With lengthscale a, timescale $(2\Omega)^{-1}$, velocity scale U, and surface displacement scale η_{00}, the non-dimensional linear shallow-water equations can be written

$$u_\tau - v = -\eta_x, \quad v_\tau + u = -\eta_y, \tag{2.1 a, b}$$

$$u_x + v_y - \epsilon \boldsymbol{\nabla} \cdot (h\boldsymbol{u}) = -\eta_\tau. \tag{2.1 c}$$

These combine to give the vorticity equation,

$$(v_x - u_y - \eta)_\tau + \epsilon \boldsymbol{\nabla} \cdot (h\boldsymbol{u}) = 0. \tag{2.2}$$

2.1. *The initial, fast, inertial adjustment* ($\epsilon \to 0$, τ *fixed*)

In the limit $\epsilon \to 0$, i.e. on the inertial timescale, topographic effects vanish from the equations. The initial conditions can be written

$$u = 0, \quad v = 0, \quad \eta = H(L - y) \quad (y \geqslant 0, \tau = 0), \tag{2.3}$$
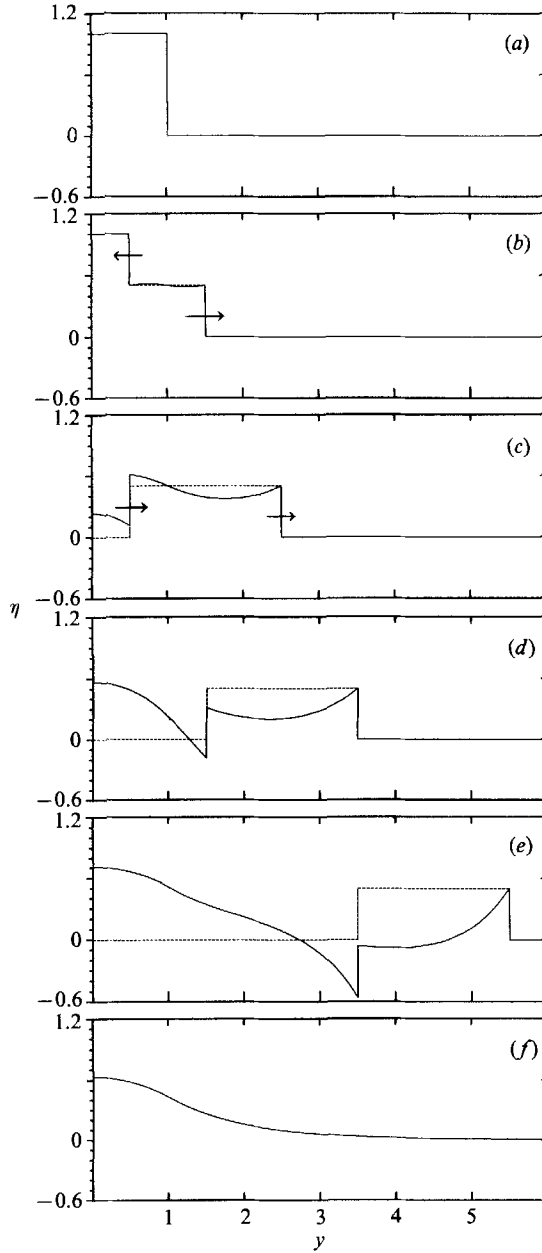
FIGURE 2. Cross-sections of surface elevation perpendicular to the wall during the initial, inertial adjustment to geostrophy. (a) $\tau = 0$, the initial step profile with $L = 1$; (b) $\tau = \frac{1}{2}L$ two fronts propagate in opposite directions away from the position of the original discontinuity; (c) $\tau = \frac{3}{2}L$, the front that initially moved inwards has reflected at the wall and now follows the other front outwards a distance $2L$ behind; (d) $\tau = \frac{5}{2}L$; (e) $\tau = \frac{9}{2}L$; (f) $\tau \to \infty$, the geostrophically adjusted surface elevation $\eta = \eta_0(y)$. The dashed curves in (b), (c), (d) and (e) show the evolution without rotation.

where $H(y)$ is the Heaviside unit function and L gives the width in Rossby radii of the initial raised section of the free surface. The impermeability condition at the wall is

$$v = 0 \quad (y = 0, \tau > 0). \tag{2.4}$$

It is sufficient to look for solutions independent of x. Then by a similar argument to Gill (1982, chapter 7), (2.1), (2.3) and (2.4) can be combined to give the forced Klein–Gordon equation

$$v_{\tau\tau} - v_{yy} + v = \delta(L - y)\,\delta(\tau), \tag{2.5}$$

where $\delta(y)$ is the Dirac delta function. The solution of (2.4), (2.5) follows by extending v to be odd about $y = 0$, by introducing the image of the forcing, to give

$$2v = J_0([\tau^2 - (y-L)^2]^{\frac{1}{2}})\,H(\tau - |y-L|) - J_0([\tau^2 - (y+L)^2]^{\frac{1}{2}})\,H(\tau - |y+L|). \tag{2.6}$$

Figure 2 gives the surface elevation for $L = 1$, obtained by integrating $\eta_\tau = -v_y$, at various times after the free surface is released. Two vertical wave fronts of amplitude one half travel at unit speed, initially in opposite directions, away from the position of the original discontinuity (figure 2b). The wavefront propagating towards the wall is reflected at the wall at time $\tau = L$ and propagates outwards a distance $2L$ behind the original outward-propagating front (figure 2c, d, e). For small τ the surface elevation evolves similarly to the solution in the absence of rotation, shown dotted in figure 2(b, c, d, e) for comparison. For large τ the effect of the Coriolis force is more evident, altering the evolution and raising permanently the surface at the wall (figure 2f).

As in the problem without a wall, at large time the flow decays as $\tau^{-\frac{1}{2}}$ towards a steady geostrophically adjusted solution. In the present geometry this steady solution can be obtained from (2.6), or directly by conservation of potential vorticity and noting that u vanishes at the wall by (2.4) since $u_\tau = v$. It thus follows from (2.2), the initial displacement (2.3) and (2.1b) that the steady adjusted flow satisfies

$$\eta_{yy} - \eta = -H(L - y) \quad (y > 0), \quad \eta_y = 0 \quad (y = 0). \tag{2.7}$$

Both the asymptotic form of (2.6) and the solution of (2.7) give $\eta \to \eta_0(y)$ as $\tau \to \infty$ where

$$\eta_0(y) = e^{-y}\sinh L + [1 - \cosh(L-y)]\,H(L-y) \quad (\tau \to \infty), \tag{2.8}$$

the profile given in figure 2(f).

2.2. *The subsequent, slow, topographic adjustment* ($\epsilon \to 0$, $t = \epsilon\tau$ *fixed*)

Now consider (2.1) in the limit $\epsilon \to 0$ on the topographic vortex-stretching timescale, i.e. with $t = \epsilon\tau$ fixed. In terms of the dimensional time t^* and the topographic timescale T, $t = t^*/T$. Then (2.1a, b) reduce to the geostrophic relations

$$u = -\eta_y, \quad v = \eta_x, \tag{2.9a, b}$$

and (2.2) gives the field equation

$$(\nabla^2\eta - \eta)_t + \partial(\eta, h) = 0 \quad (y > 0, t > 0), \tag{2.10}$$

where $\partial(\eta, h) = (\boldsymbol{u}\cdot\boldsymbol{\nabla})h = \eta_x h_y - \eta_y h_x$, relating vorticity generation and free-surface deformation to topographic compression of vortex lines. The adjusted surface displacement (2.8) gives the geostrophic initial condition

$$\eta = \eta_0(y) \quad (t = 0, y > 0), \tag{2.11}$$

required by (2.10). With (2.9b), the impermeability condition (2.4) becomes a condition that η is independent of position along the wall. In particular η is given by

its value at $x = -\infty$. Provided no waves travel with undiminished amplitude to $x = -\infty$, where the topography is taken to be flat, η is determined there for all $t > 0$ by its initial geostrophically adjusted value there, giving

$$\eta = \eta_0(0) = 1 - e^{-L} \quad (y = 0, t > 0). \tag{2.12}$$

A posteriori support for this condition comes from noting that high velocities are generated in the subsequent evolution only where the escarpment meets the wall and topographic waves are incoming. Any Poincaré waves generated in this case would spread isotropically and so have amplitude decreasing algebraically with distance. The sole constant-amplitude high-frequency wave is the Kelvin wave trapped against the wall. This wave, however, propagates in the positive x-direction only and so does not affect the surface elevation at $x = -\infty$.

Introducing the deviation from the initial geostrophically adjusted elevation, $\psi = \eta - \eta_0$, gives the problem

$$(\nabla^2 \psi - \psi)_t + \partial(\psi, h) = -\partial(\eta_0, h), \tag{2.13}$$

$$\psi = 0 \quad (y > 0, t = 0) \quad \text{and} \quad (y = 0, t > 0), \tag{2.14a, b}$$

$$\nabla \psi \to 0 \quad (x^2 + y^2 \to \infty, t > 0). \tag{2.15}$$

It is shown in Johnson (1990*a*, *b*) that the periodic response to low-frequency periodic forcing of (2.13), (2.14), (2.15) is closely modelled for ridges, valleys and escarpments by considering only the fundamental long topographic wave. For an escarpment this wave can be retained and others filtered out by taking the escarpment to be vertical. This removes short waves carrying energy away from the wall and hence corresponds to weakly dissipative flow with energy being destroyed at the wall over downwards escarpments (Johnson 1989). Since (2.13) is linear the required solution of the present initial-value problem can be expressed as a superposition of these periodic responses and hence the general features for continuous escarpments obtained by considering a vertical escarpment. Thus consider the step change in depth

$$h = \gamma \operatorname{sgn} x, \tag{2.16}$$

where $\gamma = \pm 1$ depending on whether shallow water lies to the right or left looking away from the bounding wall. Except at the step, (2.13) and (2.14*a*) give

$$\nabla^2 \psi - \psi = 0 \quad (x \neq 0, y > 0, t > 0). \tag{2.17}$$

Integrating (2.13) by parts across the step gives the matching conditions

$$[\psi] = 0, \quad [\psi_{xt}] - 2\gamma \psi_y = -2\gamma U_0, \quad (x = 0, y > 0, t > 0), \tag{2.18a, b}$$

where [.] denotes the jump in the enclosed quantity across the step and

$$U_0(y) = -\partial\eta_0/\partial y \tag{2.19}$$

is the initial cross-step velocity. Flow across the step generates a vortex sheet along the step and gives the jump in (2.18*b*). The distribution of vorticity along the step in turn alters the cross-step flow and this interaction controls wave propagation along the step.

The problem can be further simplified by looking for solutions of the form $\psi = \phi(|x|, y, t)$, where ϕ is required only in the quarter-plane $x \geq 0, y \geq 0$ where it satisfies

$$\nabla^2 \phi - \phi = 0 \quad (x > 0, y > 0, t > 0), \tag{2.20}$$

$$\phi = 0 \quad (x = 0, y > 0, t = 0) \quad \text{and} \quad (y = 0, x > 0, t > 0), \tag{2.21a, b}$$

$$\nabla\phi \to 0 \quad (x^2+y^2 \to \infty, t > 0), \tag{2.22}$$

$$\phi_{xt} - \gamma\phi_y = -\gamma U_0 \quad (x = 0, y > 0, t > 0). \tag{2.23}$$

For lengths small compared with the Rossby radius the displacement of the free surface can be neglected in the vorticity equation (2.2), and (2.20) reduces to Laplace's equation. The surface is effectively rigid, and the system becomes that solved in I by conformal mapping and Fourier transforms. The forcing appears solely through U_0, the initial cross-step flow, driven in I by a source–sink pair. Note that changing the sign of γ is equivalent to reversing the time direction.

3. The unbounded case

The difficulty in the problem posed by (2.20)–(2.23) lies in the presence of the wall. This section considers an unbounded domain first using direct Fourier-transform techniques and then using a Green's-function method that can be adapted to include a wall. Consider system (2.20)–(2.23) without (2.21 b), allowing y to extend to $-\infty$, and, for simplicity, taking the origin of y to be at the step in the free surface, so $\eta = 1 - H(y)$ before adjustment. The analysis closely parallels that in I. The initial surface displacement after geostrophic adjustment is

$$\eta_0 = \begin{cases} 1 - \frac{1}{2}e^y & (y < 0) \\ \frac{1}{2}e^{-y} & (y > 0). \end{cases} \tag{3.1}$$

3.1. *The Fourier-transform solution*

Denoting the Fourier transform with respect to y, parameter l, by $\hat{\ }$ gives

$$\hat{\eta}_0 = [\pi\delta(l) - (il)^{-1}]/(1 + l^2). \tag{3.2}$$

The form of $\hat{\phi}$ follows from (2.20) as

$$\hat{\phi} = A(l, t)\exp\{-(1 + l^2)^{\frac{1}{2}}x\}, \tag{3.3}$$

where A satisfies, from (2.23),

$$A_t + \gamma il(1 + l^2)^{-\frac{1}{2}}A = \gamma(1 + l^2)^{-\frac{3}{2}}. \tag{3.4}$$

The complementary function is a negative exponential in t (and so decays) provided the inversion contour passes below (above) the pole at $l = 0$ for γ positive (negative). This is compatible with the initial form $\hat{\eta}_0$. The steady solution of (3.4) is $A_s = [il(1 + l^2)]^{-1}$, so

$$\phi_s = -\frac{1}{2}\gamma e^{-|x|} + \frac{1}{2\pi}\int_{-\infty}^{\infty} \frac{\exp\{-(1 + l^2)^{\frac{1}{2}}|x|\}\sin ly \, dl}{l(1 + l^2)}, \tag{3.5}$$

where the integrand is well-behaved on the whole real axis, the contribution from the pole at the origin having been made explicit. For large $|y|$ the integrand is dominated by the contribution near $l = 0$ and

$$\phi_s \to \frac{1}{2}e^{-x}[\gamma + \operatorname{sgn} y] \quad (|y| \to \infty).$$

For $\gamma = 1$ the steady state has $\eta = 1$ along $x = 0$ while for $\gamma = -1$ the steady state has $\eta = 0$ along $x = 0$. There is no flow across the step in the steady solution.

The solution at intermediate times is given by

$$\eta = \eta_0 - \frac{1}{\pi}\int_0^{\infty} \frac{\exp[-(1 + l^2)^{\frac{1}{2}}|x|][\sin(ly - \omega t) - \sin ly] \, dl}{l(1 + l^2)}, \tag{3.6}$$

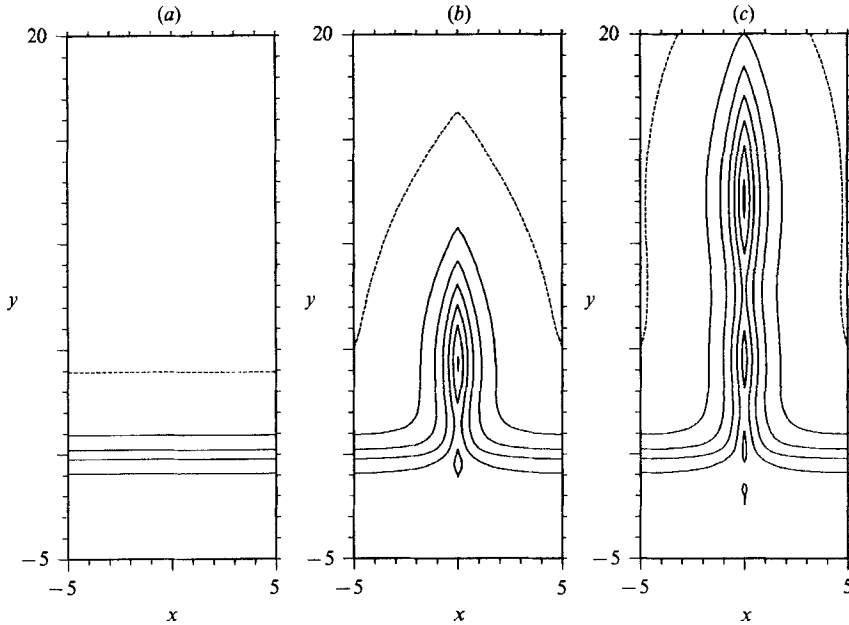FIGURE 3. Contours of surface elevation η and thus streamlines for the evolution in an infinite domain (no wall) of a step along $y = 0$ in the free surface above topography consisting of a vertical step from deep fluid in $x < 0$ to shallow fluid in $x > 0$ ($\gamma = 1$). When as here the initial surface is higher in $y < 0$ then $y > 0$ a raised tongue of fluid moves out along the escarpment, and flow is from left to right. When the initial surface is higher in $y > 0$ a valley forms along the escarpment and flow is from right to left. Eddies formed in the region of the initial step in surface elevation propagate outwards along the escarpment with shallow water to their right. (a) $t = 0, \eta = \eta_0(y)$ after initial rapid geostrophic adjustment; (b) $t = 10$; (c) $t = 20$. Contours are at 0.01 (dashed) and then at $0.2, 0.4, \ldots$.

where $\omega(l) = \gamma l(1 + l^2)^{-\frac{1}{2}}$ is the dispersion relation giving the frequency of a topographic wave of wavenumber l. The waves have phase speed $\gamma(1 + l^2)^{-\frac{1}{2}}$ and group velocity $\gamma(1 + l^2)^{-\frac{3}{2}}$. These are single-signed and thus represent unidirectional propagation of phase and energy. The integrand in (3.6) is non-singular and thus in a form for ready evaluation by fast Fourier transforms (FFTs).

Figure 3 for $\gamma = 1$ gives contours of the surface elevation, and thus streamlines, at times $t = 0$, 10 and 20 showing a raised tongue of fluid moving outwards along the escarpment. Flow is from left to right. Fluid travels outwards beside the escarpment, crosses in an unsteady front and returns on the far side. As in I, eddies form where flow approaches the escarpment and travel outwards in the tongue. In the present case the eddies remain narrow, confined by free-surface deformation.

If the sign of the initial step in surface elevation is reversed, then the sole change is a reversal of the sign of η and hence of the velocity field. The patterns of figure 3 again give the development of the flow, which in this case is a valley of fluid growing along the escarpment, with flow from right to left. If instead the sign of the topographic step is reversed ($\gamma = -1$, so the escarpment separates shallow fluid in $x < 0$ from deep in $x > 0$), then the flow pattern is reflected about $y = 0$, with respectively a valley or ridge growing into $y < 0$ when the initial surface elevation is higher or lower there.

The patterns are symmetric about $x = 0$ as the escarpment has been taken to be vanishingly small. For finite-height escarpments patterns are similar but the
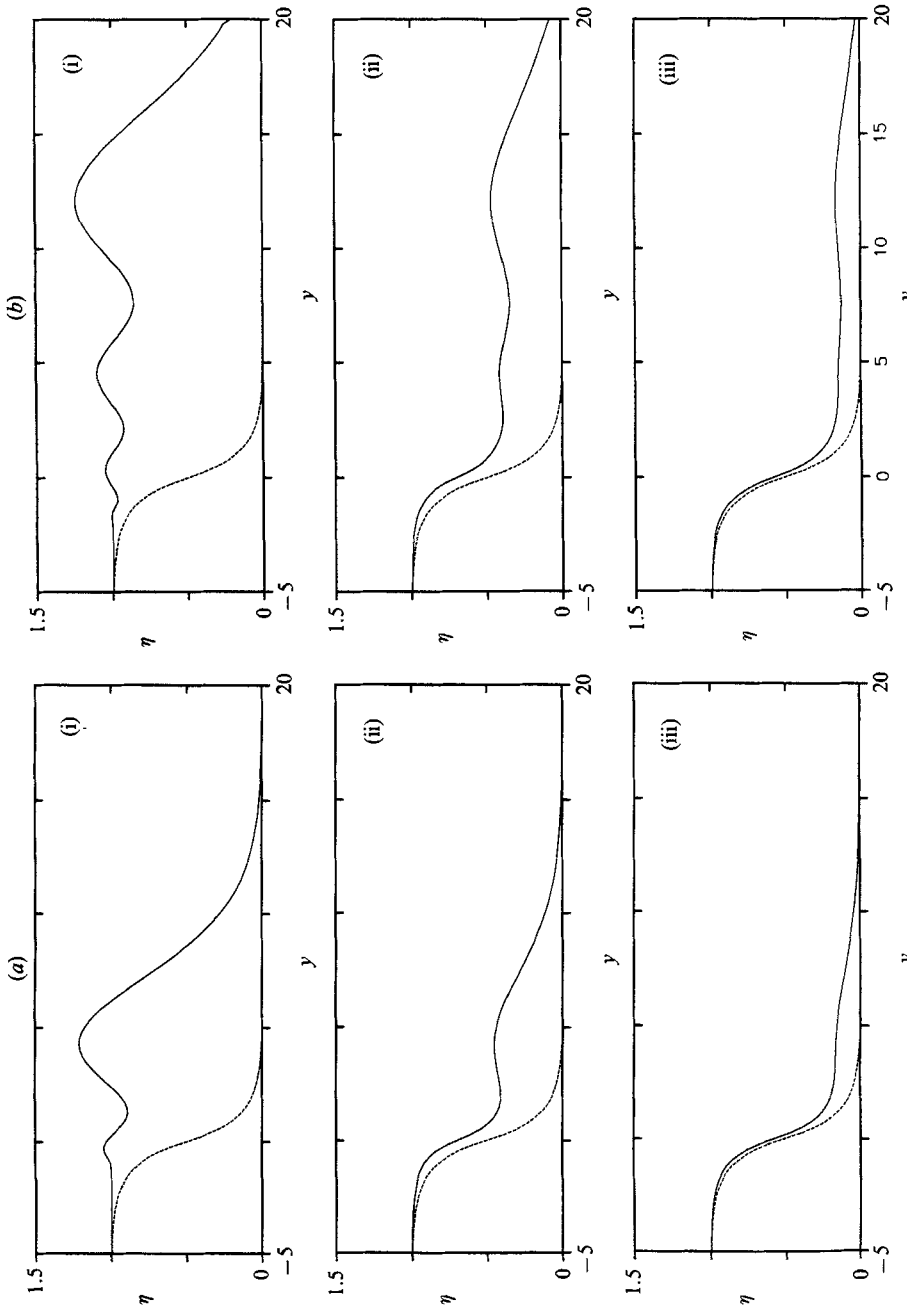
FIGURE 4. Cross-sections of surface elevation η parallel to the topographic step, for (*a*) time $t = 10$ and (*b*) $t = 20$. The cross-sections are shown at (i) $x = 0$ above the step, (ii) one Rossby radius from the step and (iii) $|x| = 2$, two Rossby radii from the step. Over the step short waves are evident in the dispersive tail behind the wavefront but they are absent away from the step owing to their rapid decay in with increasing $|x|$. The flow adjusts rapidly at any distance over a Rossby radius from the step. Displacements η_0 at $t = 0$ are shown dashed.

currents are wider on the deeper side, reflecting the larger Rossby radius there. As noted in II, continuity of interface height across the escarpment means that the outward volume flux is greater than the return flux, thus feeding the advancing front.

Asymptotic evaluation of (3.6) following I shows that the wavefront is composed of the longest waves travelling outwards with unit speed leaving behind a dispersive wavetrain decaying as $t^{-\frac{1}{2}}$. Figure 4 gives cross-sections of surface elevation at three stations in x. Short dispersive waves are evident behind the wavefront above the escarpment but are absent away from the escarpment owing to their rapid decay with $|x|$. Adjustment is thus rapid at distances over a Rossby radius from the step.

3.2. *The Green's function solution*

Although the Fourier-transform techniques and evaluation by FFTs are the most transparent and straightforward approach to wave problems in infinite domains, they are inappropriate in general for the semi-infinite geometry of (2.20)–(2.23). A Green's-function approach, that can be extended to bounded domains, is thus also presented here.

Consider the function

$$G_0(x, y, x_0, y_0) = K_0\{[(x-x_0)^2 + (y-y_0)^2]^{\frac{1}{2}}\} + K_0\{[(x+x_0)^2 + (y-y_0)^2]^{\frac{1}{2}}\}, \qquad (3.7)$$

where K_0 is the modified Bessel function of the second kind of order zero. The function G_0 consists of two free-surface point vortices at (x_0, y_0) and $(-x_0, y_0)$. Thus for $(x, y) \neq (x_0, y_0)$, G_0 satisfies (2.20), and (2.22). Further, G_0 is even in x_0 so $\partial G_0 / \partial x_0$ vanishes on $x_0 = 0$. Applying Green's theorem in the half-plane $x_0 > 0$ yields

$$\phi(x, y, t) = \frac{1}{2\pi} \int_{-\infty}^{\infty} G_0(x, y, 0, y_0) \frac{\partial \phi}{\partial x_0}(0, y_0, t)\, \mathrm{d}y_0 \quad (x \geqslant 0), \qquad (3.8)$$

where the solution has been extended to be continuous from the right at $x = 0$ so that the free-surface elevation ψ is continuous across $x = 0$ as required.† Knowledge of η_x along the line of the step determines η everywhere. Using (2.23) allows the time rate of change of (3.8) to be written as

$$\frac{\partial \eta}{\partial t}(0, y, t) = \frac{\gamma}{2\pi} \int_{-\infty}^{\infty} G_0(0, y, 0, y_0) \frac{\partial \eta}{\partial y_0}(0, y_0, t)\, \mathrm{d}y_0 \quad (t > 0) \qquad (3.9)$$

with the initial condition $\eta(0, y, 0) = \eta_0(y).$ \qquad (3.10)

This equation for η has been integrated numerically using predictor-corrector time stepping. For a time step $\Delta t = 0.1$ and a uniform grid spacing $\Delta y = 0.1$ for $-5 \leqslant y \leqslant 20$ (for $\gamma = 1$), the results are indistinguishable from those of the FFT method. The same time-stepping and integration algorithms are used in the following section for the quarter-plane problem to which no FFT solution is available.

The equivalence of expression (3.4) and the solution to (3.9) and (3.10) follows by noting that the kernel in (3.9), $2K_0(|y-y_0|)$, is of the convolution type so that the Fourier transform of (3.9) is

$$\frac{\partial \hat{\eta}}{\partial t}(0, l, t) = \mathrm{i}l(1+l^2)^{-\frac{1}{2}} \hat{\eta}(0, l, t), \qquad (3.11)$$

which, with initial condition (3.2), gives (3.5) restricted to $x = 0$.

† Morse & Feshbach (1953, pp. 801–806) briefly discuss boundary values determined by Green's functions.
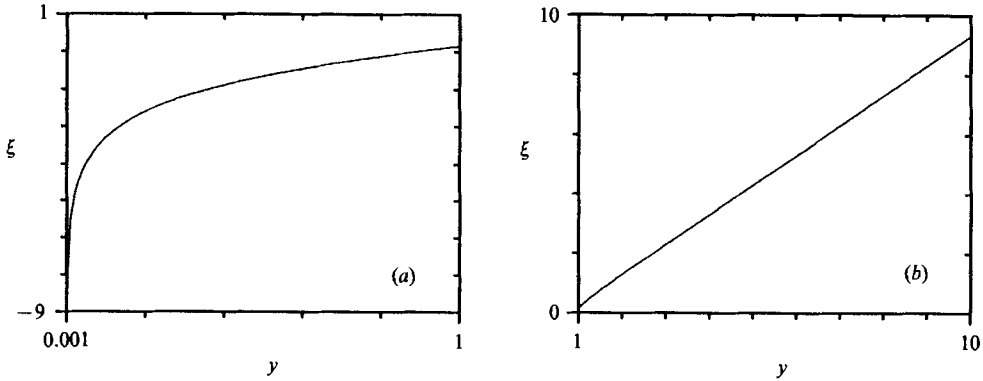
FIGURE 5. The stretched coordinate system for semi-infinite domain, $\xi = \log(\sinh y)$ so $y = \log\{e^{\xi} + (1+e^{2\xi})^{\frac{1}{2}}\}$. (*a*) Near the wall ($y \ll 1$), the scaling is exponential with $\xi \sim \log y$. (*b*) At large distances the scaling is linear with $\xi \sim y$. ($\xi = -6.9, 0.16, 9.3$ for $y = 10^{-3}, 1, 10$).
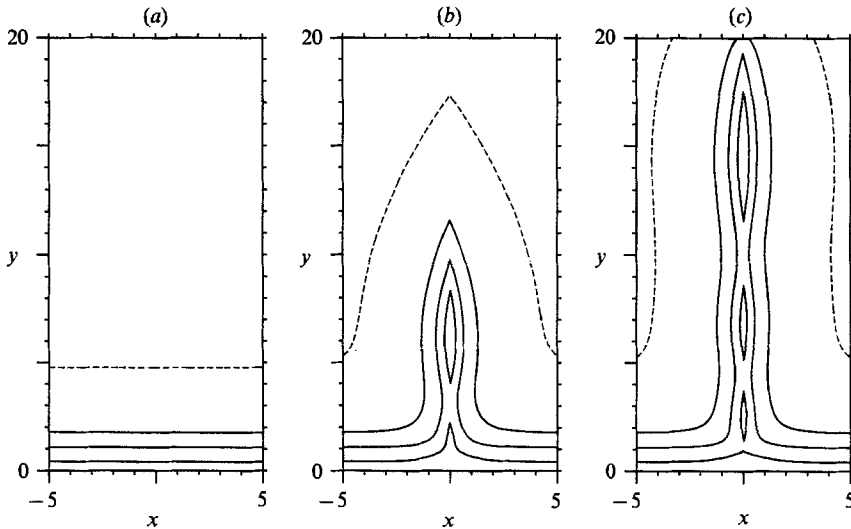

FIGURE 6. The surface elevation η for the same topography as figure 3 with, however, an impermeable wall at $y = 0$. The initial step in surface elevation is at $y = 1$. (*a*) $t = 0$, (*b*) $t = 10$, (*c*) $t = 20$. The outward-propagating eddies above the escarpment are clearly visible. The evolution of the flow is almost unaffected by the presence of the wall. The contours are at the same levels as in figure 3.

4. The wall included

The Green's-function method of the previous section extends immediately to a semi-infinite domain. Introduce the Green's function

$$G(x, y, x_0, y_0) = G_0(x, y, x_0, y_0) - G_0(x, y, x_0, -y_0), \tag{4.1}$$

consisting of the previous vortices and their images in the line $y = 0$. Then G is odd in y and so vanishes on $y = 0$. Applying Green's theorem in the quarter-plane $x \geqslant 0, y \geqslant 0$ yields

$$\phi(x, y, t) = \frac{1}{2\pi} \int_0^{\infty} G(x, y, 0, y_0) \frac{\partial \phi}{\partial x_0}(0, y_0, t) \, dy_0, \tag{4.2}$$
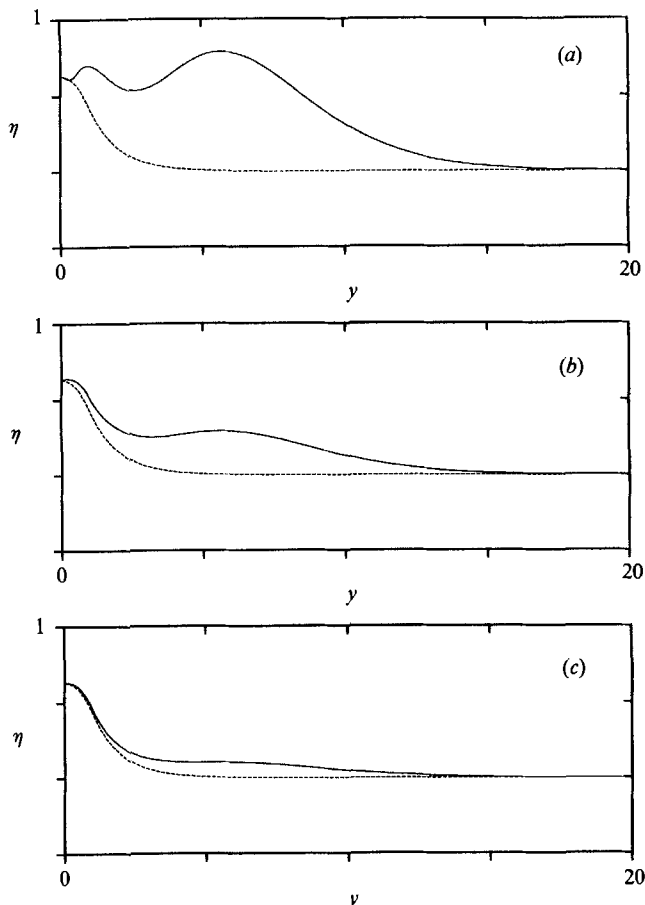
FIGURE 7. Cross-sections of the surface elevation parallel to the topographic step at $t = 10$. (a) $x = 0$, above the step, (b) one Rossby radius from the step, (c) $|x| = 2$, two Rossby radii from the step. The close resemblance to the cross-sections of figure 4 shows the negligible influence of the wall on the outgoing waves. Displacement η_0 is dashed.

and (2.23) gives the evolution equation

$$\frac{\partial \eta}{\partial t}(0, y, t) = \frac{\gamma}{2\pi} \int_0^\infty G(0, y, 0, y_0) \frac{\partial \eta}{\partial y_0}(0, y_0, t)\, \mathrm{d}y_0, \qquad (4.3)$$

with initial condition
$$\eta(0, y, 0) = \eta_0(y) \quad (y > 0). \qquad (4.4)$$

Useful information for tackling the numerical solution of (4.3) and (4.4) can be obtained from the two limit cases already studied. Far from the wall, $y \gg 1$, the second term in (4.1) is exponentially small so $G \sim G_0$ and the flow develops independently of the wall, governed by the equations of §3. The free surface can be expressed as a dispersive sinusoidal wavetrain with spatial coordinate y. Near the wall, $y \ll 1$, both terms in (4.1) are equally important. However, free-surface displacement there is negligible compared with its curvature and the rigid-lid analysis of I shows the solution to be a dispersive wavetrain in the stretched spatial
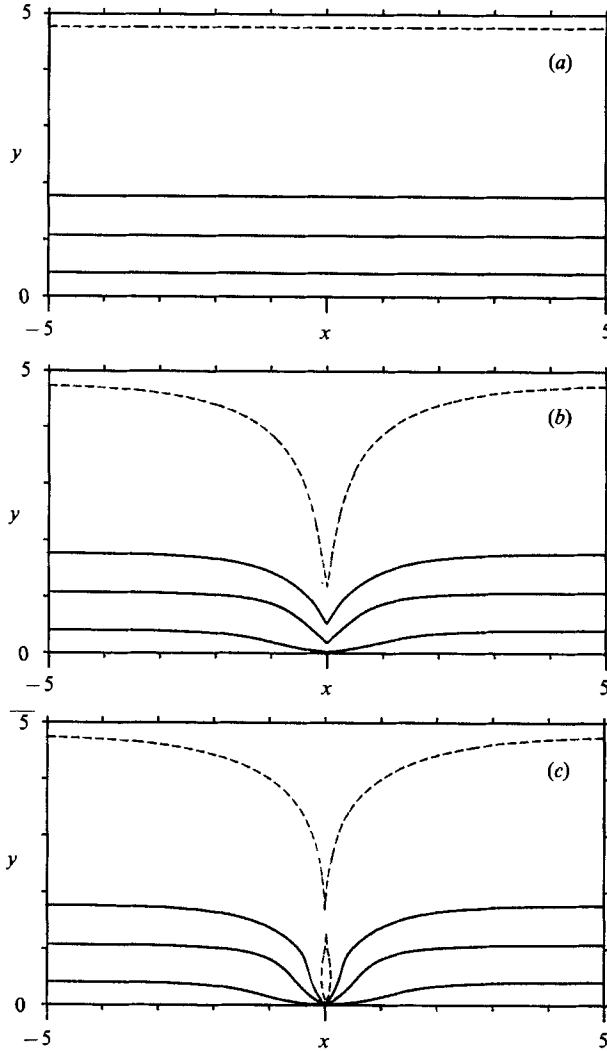
FIGURE 8. The surface elevation for the same geometry as figure 6 but for a topographic step from shallow water in $x < 0$ to deep in $x > 0$ ($\gamma = 1$). (a) $t = 0$, (b) $t = 2$, (c) $t = 5$. The wall–step singularity develops rapidly and inwardly propagating eddies closely confined to the step are clearly visible. Contours as in figure 3.

coordinate $\log y$. This follows in the present case by first integrating (4.3) by parts to give

$$\frac{\partial \eta}{\partial t}(0, y, t) = \frac{\gamma}{\pi} \int_0^\infty [K_1(|y - y_0|) + K_1(y + y_0)] \, \eta(0, y_0, t) \, \mathrm{d}y_0, \qquad (4.5)$$

and writing $\zeta = \log y$ so that

$$\frac{\partial \eta}{\partial t}(0, \zeta, t) = \frac{\gamma}{\pi} \int_{-\infty}^\infty G_1(\zeta, \zeta_0) \, \eta(0, \zeta_0, t) \, \mathrm{d}\zeta_0, \qquad (4.6)$$

where

$$G_1(\zeta, \zeta_0) = [K_1(\mathrm{e}^\zeta - \mathrm{e}^{\zeta_0}) + K_1(\mathrm{e}^\zeta + \mathrm{e}^{\zeta_0})] \, \mathrm{e}^{\zeta_0}.$$

Then in the limit $\zeta, \zeta_0 \to -\infty$ (close to the wall)

$$G_1 \to (\mathrm{e}^{\zeta - \zeta_0} - 1)^{-1} + (\mathrm{e}^{\zeta - \zeta_0} + 1)^{-1} = \operatorname{cosech}(\zeta - \zeta_0),$$
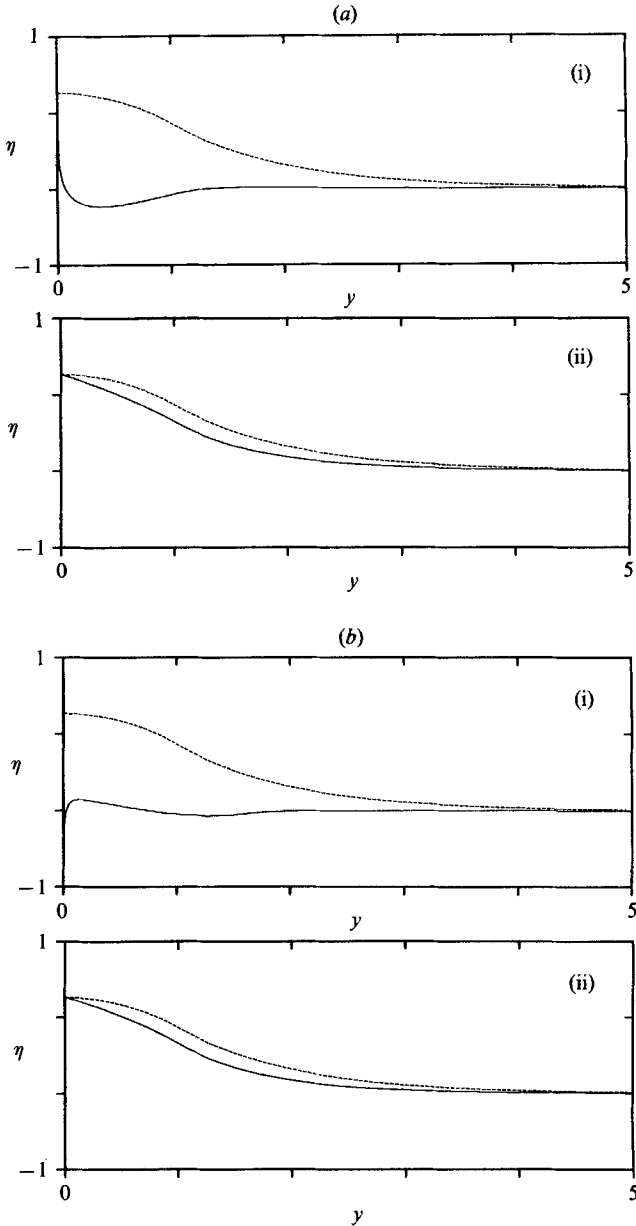
(a)

(i)

(ii)

(b)

(i)

(ii)

FIGURE 9. Cross-sections of surface elevation parallel to the topographic step. (a) $t = 5$, (b) $t = 10$. (i) Above the step the far-field condition propagates towards the wall, with a narrow time-dependent boundary-layer structure at the wall. (ii) At one Rossby radius from the step ($x = 1$) the flow alters little after $t = 1$. The dashed curves give $\eta_0(y)$.

a convolution kernel in these coordinates. The Fourier transform of (4.6) gives

$$\hat{\eta}_t = \gamma(\tanh \tfrac{1}{2}\pi k)\,\hat{\eta}, \qquad (4.7)$$

the governing equation solved directly in I.

The two cases can be combined by introducing the stretched coordinate ξ where

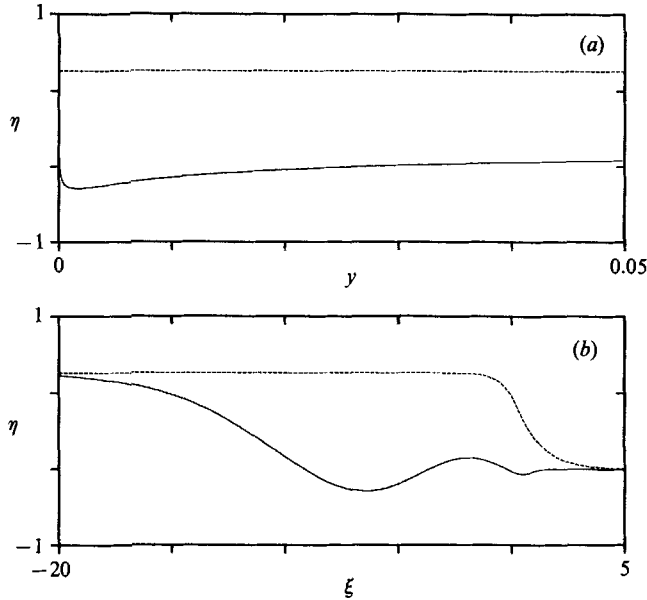$$\xi = \log(\sinh y). \qquad (4.8)$$

FIGURE 10. The surface elevation η above the topographic step at time $t = 10$ for $\gamma = -1$. (a) In the unstretched coordinate y the wavefront is indistinguishably close to the wall. (b) In the stretched coordinate ξ the wavefront is resolved. The front has just reached $\xi = -20$.

This choice has the advantage of an explicit inverse:

$$y = \log\{e^{\xi} + (1 + e^{2\xi})^{\frac{1}{2}}\}. \tag{4.9}$$

Figure 5 illustrates the stretching. For small y, figure 5(a), the stretching is exponential ($y \sim e^{\xi}$) whereas for large y, figure 5(b), the scaling is linear ($y \sim \xi$). In this scaling a wavetrain maintains an approximately constant wavelength at all distances from the wall. A grid evenly spaced in ξ gives good spatial resolution for the motion, and the time stepping of (4.3) is thus based on such a grid.

Figure 6 gives the development of the surface elevation for an outgoing wave ($\gamma = 1$), for $L = 1$. The eddies in the tongue are clearly visible. Figure 7 gives cross-sections of the elevation along three lines $x = $ constant at time $t = 10$. The rapid decay with distance perpendicular to the step of the slowly travelling short waves means that adjustment is rapid even a few Rossby radii from the step and there is little signature of the oscillatory dispersive wavetrain so evident above the step. As expected, the results differ little from those in §3 for which the wall is absent.

For an incoming wave, the steady-state flow is nipped in at a wall–step singularity as in figure 11 of II. Solving (4.3) shows how this state is effectively set up in the time taken for a topographic long wave to travel from the initial step in surface elevation at $y = L$ to the wall. Figure 8 gives the surface elevation at times $t = 0$, 2 and 5 for $L = 1$. As in the rigid-lid flow of I, eddies composed of short waves form over the step and travel inwards towards the wall. These short waves decay rapidly away from the step and once again have little effect at any distance further than a Rossby radius from the step as can be seen from the cross-sections in figure 9. On this lengthscale the wavefront has effectively reached the wall by $t = 5$. Figure 10(a) shows η along $x = 0$ close to the wall at $t = 10$. The surface displacement has not changed at the wall ($y = 0$) but now drops to a slightly negative value by $y \approx 0.01$. The velocity at the wall remains zero but a strong alongshore jet has formed close to the wall. Figure

$10\,(b)$ also shows η along $x = 0$ at $t = 10$ but now in the stretched coordinate ξ. The wavefront has just reached $\xi = -20$: for $\xi < -20$ the surface displacement remains equal to η_0. At later times the wavefront comes ever closer to the wall without actually reaching it. The time step for the numerical integration was $\Delta t = 0.2$ and the grid was equally spaced in ξ with $\Delta \xi = 0.25$ for $-20 \leqslant \xi \leqslant 5$ (i.e. $2 \times 10^{-9} \leqslant y \leqslant 5.7$).

As noted in I, as the strength of the alongshore jet increases, the initially small effects of advection and dissipation become increasingly important near the wall–step junction. Allen (1988) considers advection and obtains a finite boundary-layer width.

5. Discussion

The free-surface adjustment problem above a topographic step of II has been solved in detail numerically by reducing it to one spatial dimension and introducing the exponential scaling of I to resolve the development of the singularity at the wall–step junction. The results combine the singularity and eddies of I with the confinement due to free-surface deformation in II. In order to obtain these results in a simple form two limits have been applied to the full shallow-water equations. First, so that the initial free-surface adjustment by Poincaré and Kelvin waves is instantaneous on the topographic timescale, the fractional depth ϵ occupied by the escarpment has been taken to be vanishingly small. For higher escarpments the topographic speed increases to become comparable with the Kelvin wave speed and a solution to the present initial-value problem requires simultaneous consideration of both sets of waves. Secondly, so that advection is negligible the initial step in the free surface has been taken to be small compared with the height of the escarpment. For larger free-surface elevations stronger currents are generated by the initial Rossby adjustment and their speeds become comparable with topographic wave speeds. Advection of potential vorticity (a conserved quantity) then affects the motion. For step-like escarpments the topographic waves are unidirectional. When waves propagate away from the wall, the wall has little effect on the general flow pattern. When waves propagate towards the wall a thinning boundary layer forms near the wall–step junction together with a narrow jet of increasing velocity.

REFERENCES

ALLEN, S. 1988 Rossby adjustment over a slope. Ph.D. thesis, University of Cambridge.

GILL, A. E. 1982 *Atmosphere–Ocean Dynamics.* Academic Press, 666 pp.

GILL, A. E., DAVEY, M. K., JOHNSON, E. R. & LINDEN, P. F. 1986 Rossby adjustment over a step. *J. Mar. Res.* **44**, 713–738 (referred to herein as II).

JOHNSON, E. R. 1984 Starting flow for an obstacle moving transversely in a rapidly rotating fluid. *J. Fluid Mech.* **149**, 71–88.

JOHNSON, E. R. 1985 Topographic waves and the evolution of coastal currents. *J. Fluid Mech.* **160**, 499–509 (referred to herein as I).

JOHNSON, E. R. 1989 Boundary currents, free currents and dissipation regions in the low-frequency scattering of shelf waves. *J. Phys. Oceanogr.* **19**, 1293–1302.

JOHNSON, E. R. 1990a The low-frequency scattering of Kelvin waves by stepped topography. *J. Fluid Mech.* **215**, 23–44.

JOHNSON, E. R. 1990b Low-frequency scattering of Kelvin waves by continuous topography. *J. Fluid Mech.* (submitted).

LONGUET-HIGGINS, M. S. 1968 On the trapping of waves along a discontinuity of depth in a rotating ocean. *J. Fluid Mech.* **31**, 417–434.

Morse, P. M. & Feshbach, H. 1953 *Methods of Theoretical Physics. Part 1*. McGraw-Hill.

Rhines, P. B. 1969 Slow oscillations in an ocean of varying depth. Part 1. Abrupt topography. *J. Fluid Mech.* **37**, 161–189.

Rossby, C. G. 1937*a* On the mutual adjustment of pressure and velocity distributions in certain simple current systems. I. *J. Mar. Res.* **1**, 15–28.

Rossby, C. G. 1937*b* On the mutual adjustment of pressure and velocity distributions in certain simple current systems. II. *J. Mar. Res.* **2**, 239–263.